N. Jb. Miner. Mh.	Jg. 1985, H. 5	234–240	Stuttgart, Mai 1985

Refinement of the crystal structure of lindgrenite

By **F. C. Hawthorne** and **R. K. Eby**, Winnipeg

With 3 figures and 5 tables in the text

Hawthorne, F. C. & Eby, R. K.: Refinement of the crystal structure of lindgrenite. – N. Jb. Miner. Mh., **1985**, H. 5, 234–240, Stuttgart 1985.

Abstract: The crystal structure of lindgrenite, $Cu_3(MoO_4)_2(OH)_2$, $a = 5.394(1)$, $b = 14.023(3)$, $c = 5.608(1)$ Å, $\beta = 98.50(1)°$, $V = 419.5(1)$ Å^3, $Z = 2$, space group $P2_1/n$, has been refined to an R-index of 2.7% using 1220 observed reflections collected using graphite-monochromated MoKα X-rays. The structure consists of strips of edge-sharing $Cu\varnothing_6$ ($\varnothing$ = unspecified ligand) octahedra that are cross-linked by MoO_4 tetrahedra. Alternate strips are canted at + and – ~25° respectively to (100), the sense of the tilt being along Y. This results in close-packed layers parallel to (100). These layers are modulated along Y with an amplitude of ~1/6 of a wavelength. Such modulated layers are common in copper minerals.

Key words: Molybdate, lindgrenite, crystal structure, refinement, modulated close-packing; Chile (Chuquicamata).

Introduction

Lindgrenite is a hydroxy copper molybdate, $Cu_3(MoO_4)_2(OH)_2$ from Chuquicamata, Chile. It occurs associated with antlerite and iron oxide in massive quartz veins (Bandy, 1938), and results from the oxidation of primary molybdenite. Although only reported from this locality, it is the principal secondary molybdate mineral found here, with only isolated occurrences of wulfenite and ferrimolybdite being recorded.

Experimental

The crystals used in this work are from Chuquicamata, Chile, University of Manitoba Mineral Museum catalogue number M 5035. The crystal selected for data collection was mounted on a Nicolet R3m automated four-circle diffractometer equipped with a molybdenum-target X-ray tube and a highly oriented graphite crystal monochromator mounted with equatorial geometry. A random-orientation rotation photograph was used to locate 25 strong reflections which were automatically centred. The correct unit cell was selected from an array of real space vectors corresponding to potential unit cell axes.

0028-3649/85/1985-0234 $ 1.75

© 1985 E. Schweizerbart'sche Verlagsbuchhandlung, D-7000 Stuttgart 1

Table 1. Miscellaneous information: lindgrenite.

a =	5.394(1) Å	Crystal size (mm) =	0.14×0.21×0.27
b =	14.023(3)	Rad/Mono	Mo/Gr
c =	5.608(1)	Total Unique $\|F_o\|$	1223
β =	98.50(1)°	No. of $\|F_o\| > 4\sigma$	1220
V =	419.5(1) Å	R (observed)	2.7 %
Space group	$P2_1/n$	R_w (observed)	3.1 %

Unit cell contents: $2[Cu_3(MoO_4)_2(OH)_2]$

$R = \Sigma(|F_o|-|F_c|)/\Sigma|F_o|$

$R_w = [\Sigma w(|F_o|-|F_c|)^2/\Sigma wF_o^2]^{\frac{1}{2}}$, w = 1

Table 2. Atomic parameters for lindgrenite.

	x	y	z	$U_{equiv.}$*
Cu(1)	0	0	0	0.99(2)
Cu(2)	0.8638(1)	0.09393(4)	0.4870(1)	1.05(1)
Mo	0.45592(7)	0.15456(3)	0.87716(7)	0.86(1)
O(1)	0.9801(7)	0.2234(2)	0.4358(7)	1.9(1)
O(2)	0.6505(7)	0.0918(3)	0.1009(7)	1.8(1)
O(3)	0.5532(6)	0.1299(3)	0.5938(6)	1.5(1)
O(4)	0.1448(6)	0.1130(3)	0.8730(6)	1.4(1)
O(5)	0.1321(6)	0.0306(2)	0.3405(6)	1.0(1)
H(5)	0.27(1)	0.048(4)	0.35(1)	1.0

* $U_{equiv.} = U_{equiv.} \times 10^2$

Least-squares refinement of these reflections produced the (monoclinically constrained) cell dimensions given in Table 1, together with the orientation matrix relating the crystal axes to the diffractometer axes.

Intensity data were collected using a θ-2θ scan in 96 steps with a scan range from [2θ(MoKα_1)-1] to [2θMoKα_2)+1]° and a variable scan rate between 4.0 and 29.3°/m depending on the intensity of an initial one second count at the centre of the scan range. Backgrounds were measured for half the scan time at the beginning and end of each scan. Two standard reflections were monitored every 48 measurements to check for stability and constancy of crystal alignment. A total of 2450 reflections was measured over two asymmetric units out to a maximum 2θ of 60°. Ten strong reflections uniformly distributed with regard to 2θ were measured at 10° intervals of ψ (the aximuthal angle corresponding to rotation of the crystal about its diffraction vector) from 0–350°. These were then used to apply an empirical absorption correction to all data. The shape of the crystal was assumed to be an ellipsoid, and the lengths and orientations of the principal axes were refined to minimize the merging R index of the ψ-scan intensity data, which was reduced from 10.2 % to 2.5 %. The normal data were then corrected for absorption effects using the refined shape of the crystal, and the merging R index was 2.7 %. The data were

Table 3. Anisotropic temperature factor coefficients for lindgrenite.

	U_{11}*	U_{22}	U_{33}	U_{12}	U_{13}	U_{23}
Cu(1)	118(3)	89(3)	90(3)	−20(3)	18(3)	14(3)
Cu(2)	117(2)	75(2)	132(3)	16(2)	48(2)	12(2)
Mo	92(2)	65(2)	103(2)	0(1)	20(1)	−8(1)
O(1)	221(18)	74(15)	280(20)	9(13)	55(15)	37(13)
O(2)	200(17)	178(16)	157(16)	53(14)	−17(13)	−14(13)
O(3)	128(15)	180(16)	145(15)	12(13)	65(12)	−2(13)
O(4)	128(15)	141(15)	150(15)	−37(12)	30(12)	14(12)
O(5)	131(14)	71(13)	113(14)	−4(11)	30(11)	1(11)

* $U_{ij} = U_{ij} \times 10^4$

corrected for Lorentz, polarization and background effects, and reduced to structure factors; of the 1223 unique reflections, 1220 were classed as observed ($I > 2.5\sigma$).

Structure refinement

Systematic absences confirmed the space group $P2_1/n$ assigned by Barnes (1949). Scattering curves for neutral atoms together with anomalous dispersion coefficients were taken from Cromer & Mann (1968) and Cromer & Liberman (1970). R-indices are of the form given in Table 1 and are expressed as percentages.

Using the atomic coordinates of Calvert & Barnes (1957) as a starting model, full-matrix least-squares refinement converged rapidly to an R index of 3.9 % for an isotropic thermal model. Conversion of temperature factors to an anisotropic form and insertion of the hydrogen atom as indicated by a difference Fourier map resulted in convergence at an R index of 2.7 % and an R_w index of 3.1 % for the observed data. Final parameters are given in Tables 2 and 3, and selected interatomic distances are given in Table 4. A bond-valence analysis is offered in Table 5.

Discussion

The molybdenum cation is coordinated by four oxygens in a pseudo-tetrahedral arrangement. There is a significant difference in individual Mo−O bond lengths, and this can be interpreted as arising from the bond-valence requirements of the coordinating anions (Table 5). Other deviations from ideal tetrahedral geometry are quite small (Table 4). There are two unique Cu cations, both pseudo-octahedrally coordinated by four oxygens and two (H_2O) anions. Cu(1) lies on a centre of symmetry and the (H_2O) anions are in the *trans* configuration, whereas Cu(2) lies in a general position and the (H_2O) anions are in the *cis* configuration. Around both Cu cations, there is strong Jahn-Tel-

Table 4. Selected interatomic distances (Å) and angles (°) in lindgrenite.

Cu(1)–O(2)a, b	2.418(4)	×2	Cu(2)–O(1)	1.956(4)	
Cu(1)–O(4)c, d	1.947(4)	×2	Cu(2)–O(2)	2.298(4)	
Cu(1)–O(5)e	1.984(3)	×2	Cu(2)–O(3)	1.928(4)	
<Cu(1)–O>	2.116		Cu(2)–O(4)e	2.466(3)	
Mo–O(1)g	1.743(3)		Cu(2)–O(5)e	1.978(3)	
Mo–O(2)h	1.749(4)		Cu(2)–O(5)f	1.995(3)	
Mo–O(3)	1.779(4)		<Cu(2)–O>	2.104	
Mo–O(4)	1.774(3)				
<Mo–O>	1.761				
O(2)a–O(4)c	3.136(5)	×2	O(2)a–Cu(1)–O(4)c	91.2(1)	×2
O(2)a–O(4)d	3.072(5)	×2	O(2)a–Cu(1)–O(4)d	88.8(1)	×2
O(2)a–O(5)	2.878(5)	×2	O(2)a–Cu(1)–O(5)	81.0(1)	×2
O(2)a–O(5)e	3.361(5)	×2	O(2)a–Cu(1)–O(5)e	99.0(1)	×2
O(4)c–O(5)	2.874(5)	×2	O(4)c–Cu(1)–O(5)	93.9(1)	×2
O(4)c–O(5)e	2.685(5)	×2	O(4)c–Cu(1)–O(5)e	86.1(1)	×2
<O–O>Cu(1)	3.001		<O–Cu(1)–O>	90.0	
O(1)–O(2)	3.018(5)		O(1)–Cu(2)–O(2)	90.1(1)	
O(1)–O(3)	2.900(5)		O(1)–Cu(2)–O(3)	96.6(2)	
O(1)–O(4)e	2.925(5)		O(1)–Cu(2)–O(4)e	81.9(1)	
O(1)–O(5)e	2.898(5)		O(1)–Cu(2)–O(5)e	94.8(2)	
O(2)–O(3)	2.938(5)		O(2)–Cu(2)–O(3)	87.6(1)	
O(2)–O(5)e	2.878(5)		O(2)–Cu(2)–O(5)e	84.2(1)	
O(2)–O(5)f	3.587(5)		O(2)–Cu(2)–O(5)f	114.3(1)	
O(3)–O(4)e	3.350(5)		O(3)–Cu(2)–O(4)e	98.6(1)	
O(3)–O(5)f	2.808(5)		O(3)–Cu(2)–O(5)f	91.4(1)	
O(4)e–O(5)e	3.003(5)		O(4)e–Cu(2)–O(5)e	84.2(1)	
O(4)e–O(5)f	2.685(5)		O(4)e–Cu(2)–O(5)f	73.1(1)	
O(5)e–O(5)f	2.600(7)		O(5)e–Cu(2)–O(5)f	81.6(2)	
<O–O>Cu(2)	2.965		<O–Cu(2)–O>	89.9	
O(1)g–O(2)h	2.857(5)		O(1)g–Mo–O(2)h	109.8(2)	
O(1)g–O(3)	2.879(5)		O(1)g–Mo–O(3)	109.6(2)	
O(1)g–O(4)	2.910(5)		O(1)g–Mo–O(4)	111.7(2)	
O(2)h–O(3)	2.864(5)		O(2)h–Mo–O(3)	108.5(2)	
O(2)h–O(4)	2.852(5)		O(2)h–Mo–O(4)	108.1(2)	
O(3)–O(4)	2.895(5)		O(3)–Mo–O(4)	109.1(2)	
<O–O>Mo	2.876		<O–Mo–O>	109.5	
O(5)–H(5)	0.79(6)		Cu(1)–O(5)–H(5)	108(4)	
			Cu(2)–O(5)–H(5)	127(5)	
O(5)...O(3)	2.810(5)		Cu(2)a–O(5)–H(5)	108(4)	

a: x–1, y, z; b: 1–x, –y, –z; c: x, y, z–1; d: –x, –y, 1–z; e: 1+x, y, z; f: 1–x, –y, 1–z; g: 1/2+x, 1/2–y, 1/2+z; h: x, y, 1+z.

Table 5. Empirical bond-valence table for lindgrenite*.

	Cu(1)	Cu(2)	Mo	H(5)	Σ
O(1)		0.459	1.585		2.044
O(2)	$0.129^{\times 2}_{\downarrow}$	0.175	1.552		1.856
O(3)		0.501	1.402	0.15	2.053
O(4)	$0.472^{\times 2}_{\downarrow}$	0.114	1.426		2.012
O(5)	$0.419^{\times 2}_{\downarrow}$	0.425 0.407		0.85	2.101
Σ	2.040	2.081	5.965	1.0	

* calculated from the curves of Brown (1981); bond-valence in valence units (v. u.).

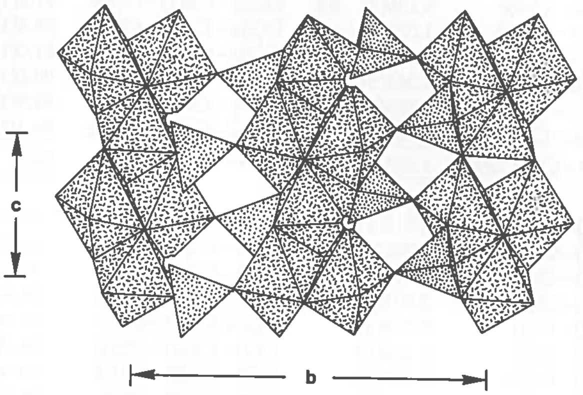

Fig. 1. The crystal structure of lindgrenite projected onto (100); $CuØ_6$ are dashed and MoO_4 tetrahedra are dotted.

ler distortion with considerable extension of the apical bonds (mean value = 2.40 Å) when compared with the equatorial bonds (mean value = 1.96 Å). Again, the wide range of bond-valences in the ($CuØ_6$) octahedra are an integral part of the satisfaction of anion bond-valence requirements; such factors affect the inter-polyhedral linkage in structures, and suggest the reason why so many Cu-minerals do not have Mg or transition-metal analogues. The hydrogen atom is bonded to O(5) and the short hydrogen bond is orthogonal to the plane of the octahedral strip (Fig. 1). There is a hydrogen bond to the O(3) anion that further promotes linkage within the structure.

A prominent feature of the lindgrenite structure are the strips of edge-sharing $CuØ_6$ (Ø = unspecified ligand) octahedra that run parallel to the Z-axis (Fig. 1). These strips are cross-linked by MoO_4 tetrahedra that share corners with the $CuØ_6$ octahedra; each MoO_4 tetrahedron links three strips together, the fourth linkage occurring along the length of one of the strips. The octahedral strips are canted at an angle of ~25° to the (100) plane, the tilt of adjacent strips (in the Y-direction) being in the opposite sense (Fig. 2).

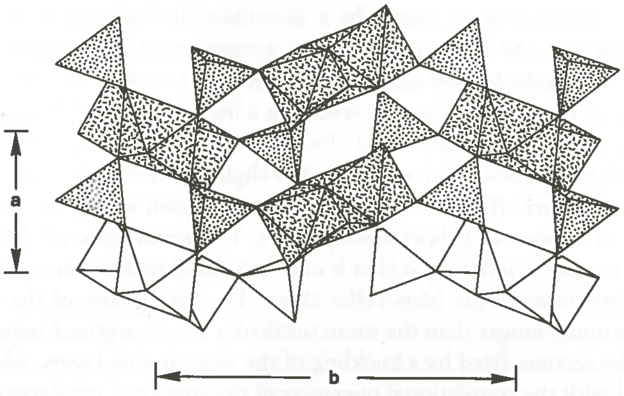

Fig. 2. The crystal structure of lindgrenite projected onto (001). One of the modulated close-packed layers is shown unshaded.

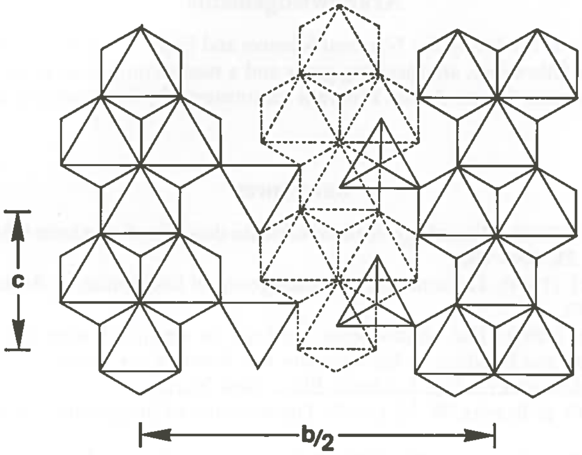

Fig. 3. An idealized close-packed layer corresponding to the (100) projection of lindgrenite (Fig. 1). An octahedral chain from the overlying layer is shown in broken lines.

Lindgrenite is actually a close-packed structure. This is not immediately obvious from inspection of the structure drawings, as the close-packed layers are not planar but are modulated such that the amplitude of the modulation is approximately equal to one sixth of the wavelength. This is illustrated in Fig. 2 by the unshaded layer of octahedra and tetrahedra. The close-packed layers are thus parallel to (100) and are modulated in the Y direction. Fig. 3 shows an ideal close-packed layer projected down X, with part of the overlying layer included to show their relative configurations. The repeat distance along Z is approximately equal to the *c* cell dimension in lindgrenite, but the repeat distance along Y is approximately twice the *b* dimension in lindgrenite. In the lindgrenite structure, the layer modulation is accompanied by a coupled rotation of the MoO_4 tetrahedra that shifts each alternate octahedra strip one half a cell-dimension in the Z-direction; this results in a halving of the *b*-dimension.

The phenomenon of modulated close-packing seems to be fairly common among copper minerals. For example, it is slightly developed in the wroewolfeite-type structures (HAWTHORNE & GROAT, 1985) and very prominent in the structure of lammerite (HAWTHORNE, 1985). The occurrence of this effect in copper minerals would suggest that it may be related to the characteristic polyhedron distortions of the Jahn-Teller effect. The axial bonds of the octahedra tend to be much longer than the mean octahedra bond lengths. Frequently this can only be accomodated by a buckling of the edge-sharing layers, which when combined with the translational operators of the structure, produces a modulation (i. e. a non-zero amplitude) in the close-packed layer.

Acknowledgements

This work was funded by the National Sciences and Engineering Research Council, in the form of a fellowship, an operating grant and a major equipment grant to F. C. H., and by the Summer Career Access Program administered by Employment and Immigration Canada.

References

BANDY, M. C. (1938): Mineralogy of three sulphate deposits of northern Chile. – Amer. Miner. **23**, 669–760.

BARNES, W. H. (1949): The unit cell and space group of lindgrenite. – Amer. Miner. **34**, 163–172.

BROWN, I. D. (1981): The bond-valence method: an empirical approach to chemical structure and bonding. – In: Structure and Bonding in Crystals, II (M. O'KEEFFE & A. NAVROTSKY, eds.). Academic Press, New York.

CALVERT, L. D. & BARNES, W. H. (1957): The structure of lindgrenite. – Can. Miner. **5**, 31–51.

CROMER, D. T. & LIBERMAN, D. (1970): Relativistic calculation of anomalous scattering factors for X-rays. – J. Chem. Phys. **53**, 1891–1898.

CROMER, D. T. & MANN, J. B. (1968): X-ray scattering factors computed from numerical Hartree-Fock wave functions. – Acta Cryst. **A24**, 321–324.

HAWTHORNE, F. C. (1985): The crystal structure of lammerite. – Acta Cryst. (submitted).

HAWTHORNE, F. C. & GROAT, L. A. (1985): The crystal structure of wroewolfeite, a mineral with $[Cu_4(OH)_6(SO_4)(H_2O)]$ sheets. – Amer. Miner. (submitted).

Manuscript received by the editor October 29, 1984, ready for print December 4, 1984.

Authors' address:

Department of Earth Sciences, University of Manitoba, Winnipeg, Manitoba R3T 2N2, Canada.